Assessment of adhesive bond strength from ultrasonic tone-bursts

John H. Cantrell

Nondestructive Evaluation Sciences Branch

NASA Langley Research Center

Hampton, Virginia 23681, USA

ABSTRACT. A model for the amplitude and phase of ultrasonic tone-bursts incident on adherend-adhesive interfaces is developed for both reflected and transmitted waves. The model parameters include the interfacial stiffness constants, which characterize the elastic properties of idealized adherend-adhesive interfaces having a continuum of bonds. The ultrasonic model is linked to the more realistic physico-chemical model of adhesive bonding via a scaling equation that establishes the relationship between the interfacial stiffness constants of the ultrasonic model and the fraction of actual bonds in the physico-chemical model. The link to the physico-chemical model enables a quantitative assessment of the absolute bond strength. The ultrasonic model and scaling equation are applied to the simulation assessment of the absolute bond strength of two aluminum alloy adherends joined by an epoxy adhesive. Model input is obtained from the calculated phase of tone-bursts reflected from the adherend-adhesive interfaces as a function of the interfacial stiffness constants. The simulation shows that the reflected phase is dominated by the first interface encountered by the incident tone-burst with little contribution from the second interface. The simulation also shows that the accuracy in assessing the adhesive bond strength depends on the sensitivity of the reflected phase to variations in the interfacial stiffness constants, reflecting in part the nonlinearity of the scaling relationship.

I. INTRODUCTION

Because of their high strength-to-weight ratio and their flexibility to meet design and manufacturing needs, composite materials such as carbon fiber reinforced polymers are being used more frequently in the aerospace and automotive industries to replace heavier metal components. Since bolting and riveting are problematic in joining two composite components, the preferred method of joining is adhesive bonding. Of critical importance is the ability of the adhesive to transfer an applied load between the joined composite adherends. The load transfer characteristics is determined by the integrity and quality of the bond between the adhesive and the adherend. Surface preparation anomalies in manufacturing may cause an adhesive bond to suffer a strength reduction or lead to an increased susceptibility of bonded interfaces to an environmental degradation while the piece is in service. Mechanisms of environmental interface degradation include loss of molecular bonds, which can result in interfacial strength reduction, the initiation and growth of micro-cracks, and eventually to failure. A quantitative nondestructive assessment of bond integrity is thus crucial to the use of joined composites in more advanced structures, especially where safety issues become more pressing.

Since ultrasound provides a direct mechanical means to interrogate bond integrity, many nondestructive techniques have centered on exploiting various properties of ultrasonic interactions with bonded interfaces to assess bond quality. Conventional ultrasonic amplitude measurements are often used to detect major interface degradation such as delaminations, but they are relatively ineffective in measuring very weak or

'kissing' bonds, since the wavelengths are generally too long compared to the thickness of the adhesive interface to provide an adequate signal-to-noise ratio. Angle beam ultrasonic spectroscopy (ABUS) [1-3] quantifies bond quality by measuring the shift in the minimum of the ultrasonic reflection frequency spectrum for both normal incidence and oblique incidence waves on bonded interfaces. Characteristic frequencies associated with adherend-adhesive interface stiffness parameters, embedded in the longitudinal and transverse ultrasonic reflection coefficients, have been used to assess bond quality [4]. Ultrasonic phase measurements have been used to assess the quality of titanium diffusion bonds [5,6]. And ultrasonic phase measurements of 'kissing bonds', simulated by dry contact interfaces, have proved promising in studies that show measurable phase shifts for different dry contacting surfaces [7]. The ability of phase measurements to assess weak and kissing bonds begs further exploration of phase-based methods for assessing the quality and integrity of adhesive bonds.

Broadband ultrasonic pulses are often used in phase measurements, where phase information is obtained from a Fourier analysis of the pulses, but phase-based methods require a high signal-to-noise ratio that is not generally achieved with broadband pulses. In contrast, measurement systems using narrow-band ultrasonic tone-bursts (gated continuous waves) generally have the necessary signal-to-noise ratio for reliable measurements. Further, ultrasonic phase-measuring systems based on constant frequency pulse phase-locked loop (CFPPLL) technology have the additional advantage that phase variations can be measured to parts in 10^9 [8]. A recent application [9] reveals that "the sensitivity of the CFPPLL instrument allows detection of bond pathologies that have been previously difficult-to-detect."

Ultrasonic measurements are based on a continuum model of adherend-adhesive interfaces where perfect adhesive bonding corresponds to an infinite array of bonds covering a finite area of adherend-adhesive contact. Realistically, the finite dimensions of atoms prevent the occurrence of an infinite array of bond sites. Adhesive bonding is more accurately described by the physico-chemical model of adhesion [10,11]. To obtain a truly quantitative assessment of adhesive bond strength a scaling equation is introduced in the present work to link ultrasonic measurements to the physico-chemical model.

The focus of the present work is to develop a model for assessing bond quality using constant frequency narrow-band phase-based techniques. Section II begins with a derivation of ultrasonic amplitude and phase contributions from adhesively bonded interfaces for normal incidence of plane waves on the bond-line. Section III shows the connection between phase-based measurements and the physico-chemical model of adhesive bond strength. Section IV applies the present model to the simulation assessment of the adhesive bond strength of two aluminum alloy 6061 adherends joined by an epoxy adhesive. Model input is obtained from the calculated phase of the reflected tone-bursts from the adherend-adhesive interfaces as a function of the interfacial stiffness constants.

II. ULTRASONIC AMPLITUDE AND PHASE CONTRIBUTIONS FROM BONDED INTERFACES

The amplitude and phase of an ultrasonic wave is derived for the case of a wave passing through adhesive material joining two monolithic structures (the adherends) of different composition. It is assumed that for gated ultrasonic continuous waves (tone-bursts) each monolithic structure can be modeled as semi-infinite and separated by the

thickness L of the adhesive joint as shown in Fig.1. The adherends are labeled (1) and (3) in Fig. 1 and the adhesive is labeled (2). For tone-bursts much longer than the thickness of the adhesive, but shorter than the thickness of either adherend, it is appropriate to consider a continuous traveling wave of displacement amplitude A_i incident from medium 1 (adherend), having mass density ρ_1 and phase velocity c_1 onto the boundary at the spatial position x = 0 between medium 1 and medium 2 (the adhesive). The adhesive has mass density ρ_2, phase velocity c_2, and thickness L. Assume a continuous wave of the form $A_i e^{-\alpha_2 x} cos(k_2 x - \omega t) = Re\left[A_i e^{-\alpha_2 x} e^{i(k_2 x - \omega t)}\right]$ propagating in medium 2, where α_2 is the attenuation coefficient in medium 2, x = 0 is the spatial position of the interface along

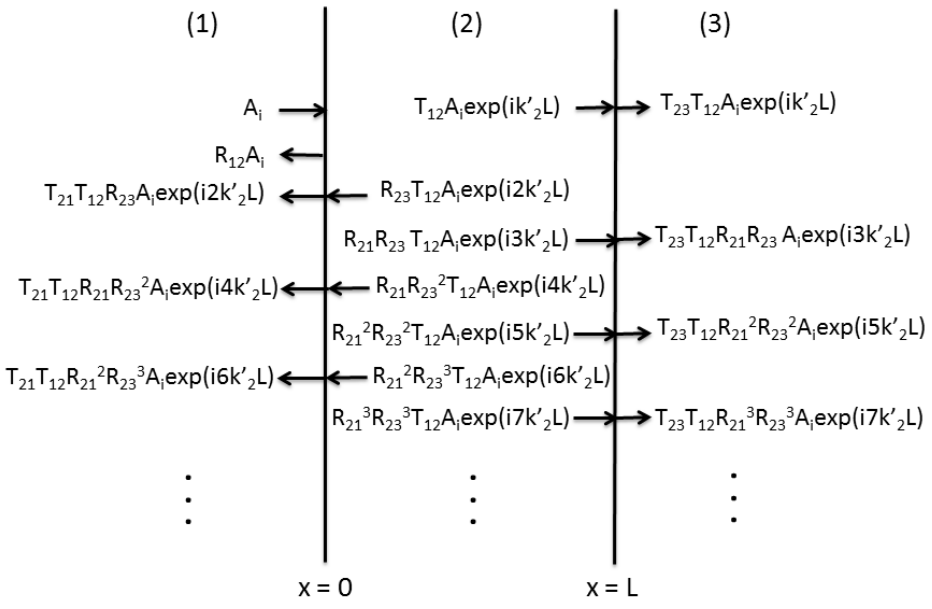

Fig.1. Schematic of acoustic wave transmission and reflection amplitudes at the boundaries x = 0 and x = L between the adhesive (medium 2) and the adherends (media 1 and 3). T_{12}, T_{21}, and T_{23} are transmission coefficients; R_{12} and R_{21} are reflection coefficients. The transmission and reflection coefficients account for imperfect bonding between the adhesive and the adherends by means of interfacial stiffness constants (see text). $k_2' = k_2 + i\alpha_2$, where k_2 is the wave number in medium 2 and α_2 is the attenuation coefficient.

the x direction between medium 1 and medium 2, ω is the angular frequency, t is time, k_2 = ω/c_2 , and c_2 is the phase velocity. The spatial position x = L corresponds to that of the interface between medium 2 and medium 3, having mass density ρ_3 and phase velocity c_3. The wave is partially reflected and partially transmitted upon each encounter with the boundaries at x = 0 and x = L. T_{12} and T_{21} are the transmission coefficients between medium 1 and medium 2, T_{23} is the transmission coefficient between medium 2 and medium 3, and R_{12} and R_{21} are the reflection coefficients between medium 1 and medium 2.

Tatersall [12] has shown that the acoustic transmission coefficient between medium *a* and medium *b* for waves incident from medium *a* is given as

$$T_{ab} = \frac{2Z_a}{Z_a+Z_b+i\omega\left(\frac{Z_aZ_b}{K_{ab}}\right)} = |T_{ab}|e^{\theta_{ab}} \qquad (1)$$

where

$$|T_{ab}| = \frac{2K_{ab}Z_a}{\left[K_{ab}^2(Z_a+Z_b)^2+(\omega Z_aZ_b)^2\right]^{1/2}} \quad , \qquad (2)$$

$$\theta_{ab} = -\tan^{-1}\frac{\omega Z_aZ_b}{K_{ab}(Z_a+Z_b)} \quad , \qquad (3)$$

$Z_a = \rho_a c_a$ is the acoustic impedance of medium *a*, ρ_a is the mass density, and c_a is the sound velocity. $Z_b = \rho_b c_b$ is the acoustic impedance of medium *b*, ρ_b is the mass density, and c_b is the sound velocity. K_{ab} is the interfacial spring stiffness constant between media *a* and *b*, and is a measure of the quality of the adhesive bond. For perfect bonds it is assumed that $K_{ab} = \infty$. Eq.(1) then reduces to the conventional transmission coefficient $T_{ab} = \frac{2Z_a}{Z_a+Z_b}$. For zero bonding it is assumed that $K_{ab} = 0$. Eq.(1) then reduces to $T_{ab} = 0$.

The reflection coefficient between medium *a* and medium *b* for waves incident from medium *a* is given as [12]

$$R_{ab} = \frac{Z_a - Z_b + i\omega\left(\frac{Z_a Z_b}{K_{ab}}\right)}{Z_a + Z_b + i\omega\left(\frac{Z_a Z_b}{K_{ab}}\right)} = |R_{ab}|e^{\phi_{ab}} \qquad (4)$$

where

$$|R_{ab}| = \left[\frac{K_{ab}^2(Z_a - Z_b)^2 + (\omega Z_a Z_b)^2}{K_{ab}^2(Z_a + Z_b)^2 + (\omega Z_a Z_b)^2}\right]^{1/2} \quad , \qquad (5)$$

and

$$\phi_{ab} = \tan^{-1}\frac{2\omega Z_a Z_b^2 K_{ab}}{K_{ab}^2(Z_a^2 - Z_b^2) + (\omega Z_a Z_b)^2} \quad . \qquad (6)$$

For perfect adhesive bonding $K_{ab} = \infty$ and Eq.(4) reduces to the conventional reflection coefficient $R_{ab} = \frac{Z_a - Z_b}{Z_a + Z_b}$. For zero bonding $K_{ab} = 0$ and Eq.(4) reduces to $R_{ab} = 1$, as expected.

As indicated in Fig.1, the wave transmitted from medium 1 through medium 2 into medium 3 is comprised of the sum of all waves transmitted into medium 3 after multiple partial reflections and transmissions between the boundaries x = 0 and x = L in medium 2. The wave transmitted into medium 3 at x = L is $A_t cos(k_3 x - \omega t) = Re\left[A_t e^{i(k_3 x - \omega t)}\right]$ where the complex transmission amplitude A_t is the sum of the complex amplitudes of waves partially transmitted into medium 3. The complex wave transmission amplitudes resulting from multiple reflections in medium 2 are shown on the right side of Fig.1, where $k_2' = k_2 + i\alpha_2$, k_2 is the wave number in medium 2 and α_2 is the attenuation coefficient.

The sum of the complex amplitudes A_t in terms of the incident wave amplitude A_i is obtained from Fig.1 as

$$\frac{A_t}{A_i} = T_{12}T_{23}e^{-\alpha_2 L}e^{ik_2 L}\sum_{n=0}^{\infty}\left(R_{21}R_{23}e^{-2\alpha_2 L}e^{i2k_2 L}\right)^n$$

$$= \frac{T_{12}T_{23}e^{-\alpha_2 L}e^{ik_2 L}}{1-R_{21}R_{23}e^{-2\alpha_2 L}e^{i2k_2 L}} = |T_t|e^{i\varepsilon} \quad . \tag{7}$$

The magnitude of the effective transmission coefficient

$$|T_t| = |T_{12}||T_{23}|e^{-\alpha_2 L}\frac{A}{B} \ , \tag{8}$$

where

$$|T_{12}| = \frac{2K_{12}Z_1}{\left[K_{12}^2(Z_1+Z_2)^2+(\omega Z_1 Z_2)^2\right]^{1/2}} \ , \tag{9}$$

$$|T_{23}| = \frac{2K_{23}Z_2}{\left[K_{23}^2(Z_2+Z_3)^2+(\omega Z_2 Z_3)^2\right]^{1/2}} \ , \tag{10}$$

$$A = \{[\cos(k_2 L + \theta_{12} + \theta_{23}) - |R_{21}||R_{23}|\exp(-2\alpha_2 L)\cos(k_2 L+\phi_{21} + \phi_{23} - \theta_{12} - \theta_{23})]^2 + [\sin(k_2 L + \theta_{12} + \theta_{23}) + |R_{21}||R_{23}|\exp(-2\alpha_2 L)\sin(k_2 L+\phi_{21} + \phi_{23} - \theta_{12} - \theta_{23})]^2\}^{1/2} \ , \tag{11}$$

$$B = 1 + |R_{21}|^2|R_{23}|^2 e^{-4\alpha_2 L} - 2|R_{21}||R_{23}|e^{-2\alpha_2 L}\cos(2k_2 L+\phi_{21} + \phi_{23}) \ , \tag{12}$$

$$|R_{21}| = \left[\frac{(Z_2-Z_1)^2K_{12}^2+\omega^2 Z_2^2 Z_1^2}{(Z_2+Z_1)^2K_{12}^2+\omega^2 Z_2^2 Z_1^2}\right]^{1/2} \ , \tag{13}$$

$$|R_{23}| = \left[\frac{(Z_2-Z_3)^2K_{23}^2+\omega^2Z_2^2Z_3^2}{(Z_2+Z_3)^2K_{23}^2+\omega^2Z_2^2Z_3^2}\right]^{1/2} \quad , \tag{14}$$

K_{12} is the interfacial spring constant between medium 1 and medium 2, K_{23} is the interfacial spring constant between medium 2 and medium 3,

$$\theta_{12} = -\tan^{-1}\frac{\omega Z_1Z_2}{K_{12}(Z_1+Z_2)} \ , \tag{15}$$

$$\theta_{23} = -\tan^{-1}\frac{\omega Z_2Z_3}{K_{23}(Z_2+Z_3)} \ , \tag{16}$$

$$\phi_{21} = \tan^{-1}\frac{2\omega K_{12}Z_2Z_1^2}{K_{12}^2(Z_2^2-Z_1^2)-\omega^2Z_1^2Z_2^2} \ , \tag{17}$$

and

$$\phi_{23} = \tan^{-1}\frac{2\omega K_{23}Z_2Z_3^2}{K_{23}^2(Z_2^2-Z_3^2)-\omega^2Z_2^2Z_3^2} \ . \tag{18}$$

The phase ε of the transmitted wave given in Eq.(7) is obtained as

$$\varepsilon = \tan^{-1}\frac{\sin(k_2L+\theta_{12}+\theta_{23})+|R_{21}||R_{23}|\exp(-2\alpha_2L)\sin(k_2L+\phi_{21}+\phi_{23}-\theta_{12}-\theta_{23})}{\cos(k_2L+\theta_{12}+\theta_{23})-|R_{21}||R_{23}|\exp(-2\alpha_2L)\cos(k_2L+\phi_{21}+\phi_{23}-\theta_{12}-\theta_{23})} \ . \tag{19}$$

The wave reflected back into medium 1 from an incident wave of amplitude A_i results from multiple partial reflections from the interfaces at x = 0 and x = L bounding medium 2. The wave reflected into medium 1 at x = 0 is $A_r cos(-k_1x-\omega t) =$

$Re\left[A_r e^{-i(k_1 x+\omega t)}\right]$ where A_r the complex reflection amplitude. The complex wave reflection amplitudes resulting from multiple reflections from the boundaries of medium 2 are shown on the left side of Fig.1. The sum of the complex reflection amplitudes A_r in terms of the incident wave amplitude A_i is obtained from Fig.1 as

$$\frac{A_r}{A_i} = R_{12}+T_{21}T_{12}R_{23}e^{-2\alpha_2 L}e^{i2k_2 L}\sum_{n=0}^{\infty}\left(R_{21}R_{23}e^{-2\alpha_2 L}e^{i2k_2 L}\right)^n$$

$$= R_{12} + \frac{T_{21}T_{12}R_{23}e^{-2\alpha_2 L}e^{i2k_2 L}}{1-R_{21}R_{23}e^{-2\alpha_2 L}e^{i2k_2 L}} = |R_r|e^{i\gamma} \qquad (20)$$

where the magnitude of the reflected wave is

$$|R_r| = \frac{\sqrt{C^2+D^2}}{1+b^2-2b\cos\Lambda}, \qquad (21)$$

$$C = a[\cos\chi - b\cos(\chi-\Lambda)] + |R_{12}|(1+b^2-2b\cos\Lambda)\cos\phi_{12}\ , \qquad (22)$$

$$D = a[\sin\chi - b\sin(\chi-\Lambda)] + |R_{12}|(1+b^2-2b\cos\Lambda)\sin\phi_{12}\ , \qquad (23)$$

$$a = |T_{21}||T_{12}||R_{23}|e^{-2\alpha_2 L}\ , \qquad (24)$$

$$b = |R_{21}||R_{23}|e^{-2\alpha_2 L}\ , \qquad (25)$$

$$\chi = 2k_2 L + \theta_{12} + \theta_{21} + \phi_{23}\ , \qquad (26)$$

$$\Lambda = 2k_2L + \phi_{21} + \phi_{23} \quad , \tag{27}$$

and the phase of the reflected wave is

$$\gamma = \tan^{-1}\frac{a[\sin\chi - b\sin(\chi-\Lambda)] + |R_{12}|(1+b^2-2b\cos\Lambda)\sin\phi_{12}}{a[\cos\chi - b\cos(\chi-\Lambda)] + |R_{12}|(1+b^2-2b\cos\Lambda)\cos\phi_{12}} \quad . \tag{28}$$

The total ultrasonic phase $\psi_{reflect}$ associated with the reflected tone-burst is

$$\psi_{reflect} = \gamma + 2(\omega/c_1)L_1 + \phi_{tdcr} \tag{29}$$

where c_1 is the sound velocity in medium 1, L_1 is the thickness of medium 1, ω is the ultrasonic angular frequency, and ϕ_{tdcr} is the phase contribution from the transducer and transducer bond. The total ultrasonic phase $\psi_{transmit}$ associated with the transmitted tone-burst is

$$\psi_{transmit} = \varepsilon + (\omega/c_1)L_1 + (\omega/c_3)L_3 + \phi_{tdcr1} + \phi_{tdcr2} \tag{30}$$

where c_3 is the sound velocity in medium 3, L_3 is the thickness of medium 3, ϕ_{tdcr1} is the phase contribution from the transmitting transducer and transducer bond, and ϕ_{tdcr2} is the contribution from the receiving transducer and transducer bond. For sufficiently thin transducer bonds the phase contribution from the transducer bonding material is relatively negligible. When operating at bonded transducer resonance the phase contribution from

the transducer is zero. Thus, when operating at bonded transducer resonance with sufficiently thin transducer bonds $\phi_{tdcr} \approx 0$.

III. CONNECTION TO PHYSICO-CHEMICAL MODEL OF ADHESIVE STRENGTH

A. The physico-chemical model

The physico-chemical model [10,11] of adhesive bond strength treats the adhesive interface as a finite array of interatomic bonds with a bond density of N bonds per unit interface area. The local tensile adhesive bond strength $\langle\sigma\rangle$ (average tensile force per unit area) is quantified by the product of the bond density N (bonds per unit area) and the average interatomic binding force per bond $\langle F\rangle$ normal to the surface as $\langle\sigma\rangle = N\langle F\rangle$. The binding force $F(r)$ of a single interatomic bond is a function of the bond interaction length r and is calculated from an interatomic potential $U(r)$ as $F(r) = -\partial U(r)/\partial r$. A commonly used potential is the Morse potential [13]

$$U(r) = U_0\left[e^{-2\mu(r-r_0)} - 2e^{-\mu(r-r_0)}\right]. \tag{31}$$

where U_0 is the bond dissociation energy, r_0 is the equilibrium separation distance between the bonded atomic pairs, and μ is the 'shape' or 'bond hardness' parameter. The maximum attractive force F_{max} occurs for $dF/dr = d^2U/dr^2 = 0$ and is obtained for $r = r' = r_0 + (1/\mu)ln2$.

The interfacial spring stiffness constant $K_{P\text{-}C}$ in the physico-chemical model is defined as $K_{P\text{-}C} = Nk$, where k is the force or 'spring' constant per interatomic bonding pair.

The spring constant k is obtained from the 'stretching' frequency ν of the bonded atoms as $k = 4\pi^2 m_r \nu^2$, where m_r is the reduced mass of the atomic pair. The frequency ν is assessed experimentally from far-infrared spectral analysis for a given pair of interacting atoms and type of bond, e.g., covalent, ionic, metallic, hydrogen, etc. [14]. The 'bond hardness' parameter is obtained as $\mu = (k/2U_0)^{1/2} = (\nu/2\pi)(m_r/2U_0)^{1/2}$.

At any given moment the adhesive interface consists of an array of N interatomic bonds per unit area with the bonds having different interaction lengths r giving rise to different interatomic forces $F(r)$. Let N_0 represent the maximum number of possible bonds per unit area of adhesive-adherend interface that occur when all possible bonds are intact and let N be the number of actual bonds per unit area that occur as the result of $(N_0 - N)$ disbonds. The disbonds result, for example, from impact damage or diffusion of moisture to the bond sites. The fraction $f = N/N_0$ of intact interatomic bonds having bond interaction lengths between r and $(r + dr)$ is assumed to follow the Weibull distribution $W(r,\delta)$ defined as [15]

$$W(r,\delta) = \frac{\pi}{2}\frac{r}{\delta^2} e^{-\frac{\pi r^2}{4\delta^2}} \tag{32}$$

where $\int_0^\infty W(r,\delta)dr = 1$ for all values of δ. The Weibull distribution is commonly used to describe systems possessing an array of parallel connections, such as that provided by the set of interatomic bonds at an adhesive-adherent interface. It is noted that the average value $\langle r \rangle$ of the interatomic interaction lengths r is given as

$$\langle r \rangle = \int_0^\infty rW(r,\delta)dr = \delta \ . \tag{33}$$

The parameter $\langle r\rangle = \delta$ is thus the average interatomic bond length in the distribution and represents the interface separation of the adhesive and adherent.

Since $\langle r\rangle = \delta$, it is assumed that the appropriate value of δ in the Weibull distribution corresponding to a separation $\langle r\rangle = r'$ is r' itself. Thus, the average interatomic binding force per bond $\langle F\rangle$ is a function of $\delta = r'$ and is obtained as

$$\langle F(\delta = r')\rangle = \int_0^\infty F(r)W(r, \delta = r')dr \quad . \qquad (34)$$

The adhesive tensile strength $\langle\sigma\rangle$ is thus calculated from the number of bonds per unit area $N = fN_0$ and Eq.(34) as

$$\langle\sigma\rangle = N\langle F(\delta = r')\rangle = fN_0\left[\int_0^\infty F(r)W(r, \delta = r')dr\right] \; . \qquad (35)$$

The evaluation of the adhesive strength $\langle\sigma\rangle$ from Eq.(35) requires that an assessment of the fraction f of intact bonds be assessed experimentally and that $\delta = r'$ be calculated for the bond separation distance $r' = r_{max} = r_0 + (1/\mu)ln2$, corresponding to the maximum value of $F(r) = -dU/dr$. These assessments are discussed in Section IIIB for the case of aluminum-epoxy bonds.

B. Scaling between the ultrasonic and physico-chemical models of interface bonding

Eq.(35) shows that the tensile adhesive bond strength $\langle\sigma\rangle$ can be calculated in the physico-chemical model from the product of the number of intact bonds $N = fN_0$ and the average interatomic binding force per bond $\langle F(\delta = r')\rangle$. It is noted that the product

involves an assessment of the interface separation distance $r' = \delta = \langle r \rangle$. The maximum value of $F(r)$ is obtained for an interatomic separation distance of $r' = r_{max} = \delta_{max} = r_0 + (1/\mu)ln2$. Evaluation of $(r_0 + (1/\mu)ln2)$ requires knowledge of the types of bonding between the adherend and the adhesive. For definiteness, consider adhesive bonding between an aluminum adherent and an epoxy adhesive.

The bonding between an aluminum adherent and an epoxy adhesive is dominated by hydrogen bonds that occur between alumina surfaces (resulting from exposure of aluminum to atmospheric moisture) and epoxy molecules. The alumina surfaces are terminated by a monolayer of hydroxyl (OH) groups with an area density of roughly 1.25 x 10^{19} OH m^{-2} [16]. The OH groups are strongly bound via Al-O bonds to the alumina and provide a hydrogen bond (H-bond) donor function for chemical bonding to H-bond receptor groups B in the epoxy. The equilibrium separation distance r_0 of the H--B bonds is roughly 1.7 x 10^{-10} m, the parameter μ = 3.6 x 10^9 m^{-1}, the dissociation energy U_0 is of the order 4.93 x 10^{-20} J per bond, and the reduced mass m_r=1.63 x 10^{-27} kg [16]. Thus, $r' = r_{max} = \delta_{max} = r_0 + (ln2/\mu) =$ 3.63 x 10^{-10} m. From the relation $\nu = (1/2\pi)\,(k/m_r)^{1/2}$ the spring constant k is calculated to be k =1.3 N m^{-1}. The maximum average interatomic binding force per bond $\langle F \rangle_{max}$ is calculated from Eqs.(31), (34), and the relation $\langle F \rangle = -\langle dU/dr \rangle$, using the value $\delta = r' = r_{max}$ = 3.63 x 10^{-10} m, to obtain $\langle F \rangle_{max} = \langle F(\delta = r') \rangle = -3.74\, x10^{-11}$N.

The maximum number of bond per unit area N_0 can be assessed from the relation [11]

$$N_0 = \frac{1}{\alpha^2}\left(\frac{M_{rep}}{M_{epox}}\right)\left(\frac{\rho_{epox} N_A}{M_{rep}}\right)^{2/3} \qquad (36)$$

where M_{epox} = 3200 is the molecular weight of epoxy molecules, M_{rep} = 340 is the molecular weight of the repeat unit of the epoxy molecule, ρ_{epox} = 1.3. x 10^3 kg m^{-3} is the mass density of epoxy, N_A = 6.02 x 10^{23} molecule/mole is Avogadro's number, and α is a factor to account for the interpenetration of epoxy molecular chains. Assuming that α = 0.05 (corresponding to a moderate to high degree of molecular interpenetration) leads to the maximum bond density value N_0 = 7.4 x 10^{17} m^{-2}. The value of N_0 and the value k =1.3 N m^{-1}, calculated above, lead to an assessment of the maximum interfacial spring stiffness constant $(K_{P\text{-}C})_{\max}$ in the physico-chemical model as $(K_{P\text{-}C})_{\max} = N_0 k$ = 9.6 x 10^{17} N m^{-3}. The value of N_0 and the value $\langle F(\delta = r')\rangle = -3.74 \times 10^{-11}$N for the interatomic bond force lead to the assessment of the maximum bond strength $\langle\sigma\rangle_{max} = 28$ MPa. This value is in very good agreement with the range (21–52) MPa typically measured for the tensile bond strengths of aluminum-epoxy bonding. The larger values of adhesive bond strength correspond to surface treatments that promote greater molecular chain interpenetration in the adhesive, which lead to smaller values of α in Eq. (36) [17,18]. Treatments affecting the specificity of the adhesive functional groups to promote covalent bonding also increase the adhesive bond strength [17,18]. In view of the variety of treatments available that affect adhesive bonding the calculated value $\langle\sigma\rangle_{max} = 28$ MPa is in quite good agreement with the results of experiment.

Before addressing experimental measurements of the fraction of intact bonds f in the physico-chemical model, it is important to point out that the equations derived in Section II are an idealization of the adhesive interface based on continuum mechanics, where the maximum number of possible bonds per unit area of interface is considered to be infinite. Perfect interface adhesion in such case corresponds to an infinite bond density

and results in an infinite interfacial spring stiffness constant K_{ab} (i.e., that $K_{ab} = \infty$). For a totally fractured interface the bond density is zero and leads to $K_{ab} = 0$. Realistically, the maximum number N_0 of possible bonds per unit area of interface in the physico-chemical model is limited by the finite dimensions of the bonded atomic pairs. To relate the ultrasonic model given in Section II to the physico-chemical model of adhesive bond strength it is necessary to scale the value of the interfacial spring stiffness constant K_{ab} in the ultrasonic model to the fraction of intact bonds $f = N/N_0$ in the physico-chemical model and thus to the interfacial spring stiffness constant $K_{P\text{-}C} = Nk = fN_0k$ for the physico-chemical model.

The scaling between the interfacial spring stiffness constant K_{ab} in the ultrasonic model and the interfacial spring stiffness constant $K_{P\text{-}C}$ in the physico-chemical model can be accomplished by writing

$$K_{ab} = \frac{f}{1-f} N_0 k = \frac{f}{1-f} (K_{P-C})_{max} = \frac{K_{P-C}}{1-f} \quad . \tag{37}$$

where $K_{P\text{-}C} = Nk = fN_0k = f\,(K_{P\text{-}C})_{\max}$. For complete fracture the fraction of intact bonds $f = 0$ in Eq.(37) and $K_{ab} = K_{P\text{-}C} = 0$. With increasing f, K_{ab} increases monotonically in Eq.(37), attaining the value $K_{ab} = \infty$ for maximum bonding at $f = 1$, where the maximum value of $K_{P\text{-}C}$ is $(K_{P\text{-}C})_{\max} = N_0k$, in agreement with the ultrasonic model. Eq.(37) thus represents a realistically scaled mapping of the interfacial spring stiffness constant between the physico-chemical model and ultrasonic continuum model of adhesion. The mapping allows a quantitative assessment of the adhesive bond strength from ultrasonic phase measurements.

IV. ULTRASONIC PHASE MEASUREMENTS AND ASSESSMENT OF ADHESIVE BOND STRENGTH

As noted in Section II, the assessment of the fraction of intact bonds $f = N/N_0$ must be obtained experimentally. One means of assessing f is from measurements of the ultrasonic phase resulting from bonded surfaces. Ultrasonic amplitude measurements can also be used, but phase measurements are considerably more accurate, since phase measurements are based on highly accurate frequency standards. Ultrasonic phase-measuring systems based on constant frequency pulse phase-locked loop (CFPPL) technology can yield phase measurements to parts in 10^9 [8].

To evaluate the effectiveness of the present model for the assessment of adhesive bond strength, it is necessary to focus only on the phase contributions from the bonded region. Contributions from outside that region simply add terms readily calculated from knowledge of the thickness, ultrasonic velocity and attenuation of the adherends. It is instructive to begin with the somewhat idealized case of identical adherends bonded with an adhesive of thickness L and having identically bonded adhesive-adherend interfaces such that $K_{12} = K_{23} = K$. In such case $|R_{21}| = |R_{12}| = |R_{23}|$, $\phi_{21} = \phi_{23}$, $|T_{21}| = |T_{23}|$, and $\theta_{21} = \theta_{12} = \theta_{23}$. For definiteness, it is assumed that the adherends are aluminum alloy 6061 (AA6061) and that the adhesive is epoxy. The density of AA6061 is 2.68×10^3 kg m^{-3} and the velocity is 6.43×10^3 m s^{-1}. The density of epoxy is 2.53×10^3 kg m^{-3} and the velocity is 2.14×10^3 m s^{-1}. An ultrasonic frequency of 10 MHz and an epoxy adhesive thickness $L = 7.6 \times 10^{-5}$ m are assumed. The reflected ultrasonic phase γ is calculated from

Eq.(28). A graph of the phase of the reflected ultrasonic wave is plotted in Fig.2 as a function of the interfacial spring constant $K_{12} = K_{23} = K$.

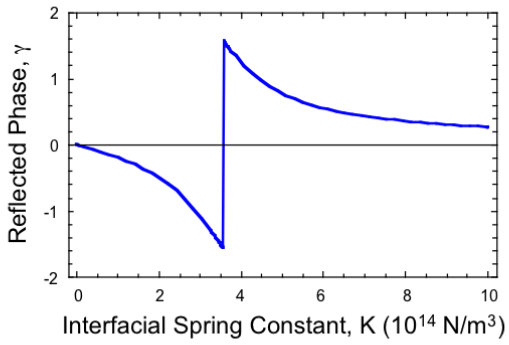

Fig.2. Graph of the phase γ of the ultrasonic wave reflected from the adherend-adhesive region plotted as a function of the interfacial spring constant $K_{12} = K_{23} = K$.

It is noted from Fig.2 that for an ultrasonic interfacial spring constant value of roughly $K = 3.5\ x\ 10^{14}$ N m^{-3} the reflected phase changes signs. The maximum value of $K_{P\text{-}C}$ in the physico-chemical model for aluminum-epoxy bonding is calculated in Section IIIB to be $(K_{P-C})_{max} = N_0 k = 9.6\ x\ 10^{17}$ N m^{-3}. Substituting $(K_{P-C})_{max}$ and $K_{ab} = K = 3.5\ x\ 10^{14}$ N m^{-3} in Eq.(37) and solving for f yields the fraction of intact bonds $f = 3.6\ x\ 10^{-4}$. The value $K = f N_0 k = 3.5$ x 10^{14} N m^{-3} thus corresponds to an adhesive strength of $\langle\sigma\rangle = f N_0 \langle F\rangle_{max} = 10$ kPa, which is almost four orders of magnitude below the maximum adhesive strength calculated in Section IIIB of $\langle\sigma\rangle_{max} = N_0 \langle F\rangle_{max} = 28$ MPa. An adhesive strength of 10 kPa is effectively an adhesive bond failure.

It is important to note from Fig.2 that since the phase changes sign at $K = 3.5\ x\ 10^{14}$ N m^{-3}, the relationship between γ and K is single-valued. This means that there

is no ambiguity in assessing the value of K from a measurement of the ultrasonic phase γ. Further, a measured negative value of the reflected phase means the adhesive bond has failed, since a negative value means that the bond strength is below 10 kPa. Thus, 'kissing bonds' are detected as a negative phase.

The general procedure to assess the adhesive bond strength from a measurement of the ultrasonic phase γ is to substitute the measured value of γ in Eq.(28) and solve for the interfacial stiffness constant K. The calculated value of $K = K_{ab}$ is then substituted in Eq.(37) and solved for the fraction of intact bonds $f = N/N_0$. The assessment of the bond strength is then calculated from the relation $\langle\sigma\rangle = f N_0 \langle F\rangle_{max}$ obtained from the physico-chemical model. The calculations leading to quantitative values of the bond strength require a detailed knowledge of the physical and dimensional properties of the adherend and adhesive, as well as the type of chemical bonds between the bonding atomic pairs. It is noted that for large values of K, corresponding to strong adhesive strength, the rate of change in γ with respect to K, dγ/dK, becomes increasingly smaller. Since perfect bonding corresponds to $K \rightarrow \infty$ such that $f \rightarrow 1$ and $K_{P\text{-}C} \rightarrow (K_{P\text{-}C})_{max}$, the evaluation of the bond strength for the strongest bonds becomes more difficult to ascertain as K becomes ever larger. However, the ability of CFPPLL-based ultrasonic instrumentation to measure phase to parts in 10^9 [8] allows state-of-the-art capability for such assessments.

It is assumed in obtaining Fig.2 that the two adherend-adhesive interfaces are identical such that the interfacial spring constants $K_{12} = K_{23} = K$. Generally, this is not the case. Fig.3 shows a graph of the reflected ultrasonic phase γ, Eq.(28), plotted as a function of K_{12} and K_{23}. It is seen that γ depends dominantly on K_{12} with very little dependence on K_{23}. This means that measurements of the reflected ultrasonic phase primarily provide

information on the first adherend-adhesive interface encountered by the ultrasonic tone-burst. Information on the second adherend-adhesive interface requires that reflected phase measurements be obtained from tone-bursts incident from the opposite adherend.

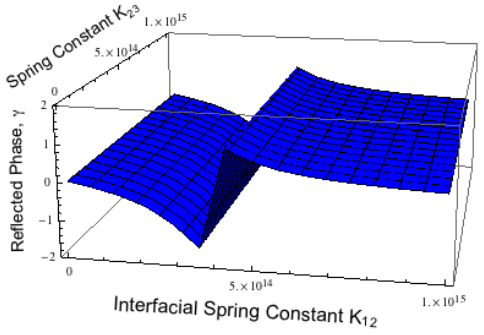

Fig.3. Graph of the phase γ of the ultrasonic wave reflected from the adherend-adhesive region plotted as a function of the interfacial spring constants K_{12} and K_{23}.

V. CONCLUSION

A model of ultrasonic tone-bursts incident on adherend-adhesive interfaces is developed for assessing the amplitude and phase of both reflected and transmitted waves. The model parameters include the ultrasonic frequency, the acoustic impedances of the adherends and the adhesive, and the interfacial stiffness constants of the adherend-adhesive interfaces. The interfacial stiffness constants characterize the elastic properties of the interfacial bonds. The ultrasonic model intrinsically assumes an idealized interface based on the continuum mechanics approximation, where the maximum number of possible

bonds per unit area of interface is considered to be infinite. Perfect interface adhesion in such case corresponds to an infinite bond density and results in an infinite interfacial spring stiffness constant K_{ab}. For a totally fractured interface the bond density is zero and leads to a null value of K_{ab}.

Realistically, the maximum number N_0 of possible bonds per unit area of interface is limited by the finite dimensions of the bonded atomic pairs. The limitation led previously to the development of the physico-chemical model of adhesive bonding [10,11]. To relate the present ultrasonic model to the physico-chemical model of adhesive strength a scaling equation is introduced that links the interfacial spring stiffness constant K_{ab} in the ultrasonic model to the fraction of intact bonds $f = N/N_0$ (N = number of intact bonds) in the physico-chemical model and thus to the interfacial spring stiffness constant $K_{P\text{-}C} = fN_0k$ (k = interatomic force constant) in in the physico-chemical model. The link establishes the connection between ultrasonic measurements of amplitude and phase, and the interatomic bonding parameters in the physico-chemical model. The link thus provides a means of calculating the tensile adhesive bond strength from knowledge of the types of bonds (e.g. H-bonds, covalent bonds, etc.) and the physical parameters of the bonds (such as bond dissociation energy, the equilibrium distance between bonded atomic pairs, and 'bond hardness' parameter).

The present model is applied to the simulation assessment of the adhesive bond strength of two AA 6061 adherends bonded with an epoxy adhesive. The simulation is obtained for the phase of a 10 MHz ultrasonic tone-burst reflected from the adherend-adhesive interfaces. It is shown that the phase changes sign for an ultrasonic interfacial stiffness constant $K = K_{ab}$ = 3.5 x 10^{14} N m^{-3}, which corresponds to a bond strength of 10

kPa as assessed from the physico-chemical model. This is well below the maximum tensile bond strength of 28 MPa, corresponding to $(K_{P-C})_{max} = N_0 k = 9.6\,x\,10^{17}$ N m^{-3}. Above 10 kPa the phase is positive and below it is negative. It is also shown that measurements of the reflected ultrasonic phase primarily provide an assessment of the bond strength of the first adherend-adhesive interface encountered by the ultrasonic tone-burst. An assessment of the second adherend-adhesive interface requires that reflected phase measurements be obtained from tone-bursts incident from the opposite adherend.

For large values of *K* the rate of change in γ with respect to *K* becomes increasingly smaller. Perfect adhesive bonding corresponds to $K \rightarrow \infty$ such that $f \rightarrow 1$ and $K_{P-C} \rightarrow (K_{P-C})_{max}$. Thus, the quantitative evaluation of the adhesive bond strength for the strongest bonds becomes more difficult to ascertain as *K* becomes ever larger. However, the difficulty is greatly mitigated by the state-of-the-art capability of CFPPLL-based ultrasonic instrumentation to measure phase to parts in 10^9 [8].

ACKNOWLEDGMENT

This research was supported in-house by the Advanced Composites Program, NASA Langley Research Center, Hampton, Virginia, USA.

REFERENCES

1. I. Lavrentyev, S. I. Rokhlin. 1997. "Determination of Elastic Moduli, Density, Attenuation, and Thickness of a Layer Using Ultrasonic Spectroscopy at Two Angles," *Journal of the Acoustical Society of America,* 102(6):3467-3477.

2. S. I. Rokhlin, L. Wang, B. Xie. 2004. "Modulated Angle Beam Ultrasonic Spectroscopy

for Evaluation of Imperfect Interfaces and Adhesive Bonds," *Ultrasonics,* 42:1037-1047.

3. L. Adler, S. Rokhlin, C. Mattei, G. Blaho, and Q. Xie. 1999. "Angle Beam Ultrasonic Spectroscopy System for Quantitative Inspection of Adhesive Bonds," in *Review of Progress in Quantitative Nondestructive Evaluation,* edited by D. O. Thompson and D. E. Chimenti (Kewar Academic/Plenum, 1999); Vol. 18, p.1553.
4. P. B. Nagy. 1991. "Ultrasonic Detection of Kissing Bonds at Adhesive Interfaces," *Journal of Adhesion Science and Technology,* 5(8):619-630.
5. K. Milne, P. Cawley, P. B. Nagy, D. C. Wright, A. Dunhill. 2011. "Ultrasonic Non-Destructive Evaluation of Titanium Diffusion Bonds," *Journal of Nondestructive Evaluation,* 30:225-236.
6. E. Escobar-Ruiz, D. C. Wright, I. J. Collison, P. Cawley, P. B. Nagy. 2014. "Reflection Phase Measurements for Ultrasonic NDE of Titanium Diffusion Bonds," *Journal of Nondestructive Evaluation,* 33:535-546.
7. J. Krolikowski, J. Szczepek. 1992. "Phase Shift of the Reflection Coefficient of Ultrasonic Waves in the Study of the Contact Interface," *Wear,* 157:51-64.
8. W. T. Yost, J. H. Cantrell, P. W. Kushnick. 1992. "Fundamental Aspects of Pulse Phase-Locked Loop Technology-based Methods for Measurement of Ultrasonic Velocity," *Journal of the Acoustical Society of America,* 91(3):1456-1468.
9. H. Haldren, A., D. F. Perey, W. T. Yost, K. E. Cramer, M. C. Gupta. 2016. "Nondestructive Evaluation of Adhesive Bonds via Ultrasonic Phase Measurements," in *Proceedings of the 31st Annual Technical Conference of the American Society for Composites,* Williamsburg, Virginia, USA 19 - 22 September 2016: 1716-1730.

10. J. H. Cantrell. 2004. “Determination of Absolute Bond Strength from Hydroxyl Groups at Oxidized Aluminum-Epoxy Interfaces by Angle Beam Ultrasonic Spectroscopy,” *Journal of Applied Physics,* 96(7):3775-3781.
11. J. H. Cantrell. 2015. “Hydrogen Bonds, Interfacial Stiffness Moduli, and the Interlaminar Shear Strength of Carbon Fiber-Epoxy Matrix Composites,” *AIP Advances,* 5:037125.
12. H. G. Tattersall. 1973. “The Ultrasonic Pulse-Echo Technique as Applied to Adhesion Testing,” *Journal of Physics D: Applied Physics,* 6:819-832.
13. A. Kelly, N. H. Macmillan. 1986. *Strong Solids* (Clarendon, Oxford, 1986), p. 7.
14. H. Knözinger. 1976. “Recent Developments in Theory and Experiments,” in *The Hydrogen Bond*, edited by P. Schuster, G. Zundel, and C. Sandorfy (North-Holland, Amsterdam, 1976), pp. 126.
15. Z. P. Bažant, S. D. Pang. 2007. “Activation Energy Based Extreme Value Statistics and Size Effect in Brittle and Quasibrittle Fracture,” *Journal of the Mechanics and Physics of Solids*, *55*(1): 91-131.
16. M. D. Joesten, L. D. Schad. 1974. *Hydrogen Bonding* (Dekker, New York,1974).
17. V. Pocius. 2002. *Adhesion and Adhesives Technology* (Hauser, Munich, 2002).
18. S. Wu. 1982. *Polymer Interfaces and Adhesion* (Dekker, New York, 1982).